

## Strong screening in the plum pudding model

This article has been downloaded from IOPscience. Please scroll down to see the full text article.

2011 EPL 94 68010

(<http://iopscience.iop.org/0295-5075/94/6/68010>)

View [the table of contents for this issue](#), or go to the [journal homepage](#) for more

Download details:

IP Address: 193.54.88.99

The article was downloaded on 29/06/2011 at 11:41

Please note that [terms and conditions apply](#).

## Strong screening in the plum pudding model

A. D. CHEPELIANSKII<sup>1</sup>, F. CLOSA<sup>2</sup>, E. RAPHAËL<sup>2</sup> and E. TRIZAC<sup>3</sup>

<sup>1</sup> *LPS, UMR CNRS 8502, Bât. 510, Université Paris-Sud - 91405 Orsay, France, EU*

<sup>2</sup> *Gulliver, UMR CNRS 7083, ESPCI - 10 rue Vauquelin, 75005 Paris, France, EU*

<sup>3</sup> *Université Paris-Sud, Laboratoire de Physique Théorique et Modèles Statistiques, UMR CNRS 8626 91405 Orsay, France, EU*

received 26 January 2011; accepted in final form 3 May 2011

published online 13 June 2011

PACS 82.70.Dd – Colloids

PACS 52.27.Gr – Strongly-coupled plasmas

PACS 05.20.Jj – Statistical mechanics of classical fluids

**Abstract** – We study a generalized Thomson problem that appears in several condensed matter settings: identical point-charge particles can penetrate inside a homogeneously charged sphere, with global electro-neutrality. The emphasis is on scaling laws at large Coulombic couplings, and deviations from mean-field behaviour, by a combination of Monte Carlo simulations and an analytical treatment within a quasi-localized charge approximation, which provides reliable predictions. We also uncover a local overcharging phenomenon driven by ionic correlations alone.

Copyright © EPLA, 2011

The venerable Thomson problem of finding the ground state of an ensemble of electrons confined in a homogeneously charged neutralizing sphere, is still unsolved and has a long history, see, *e.g.*, [1–3] and references therein for the different generalizations that have been put forward. The model was introduced at the beginning of the 20th century [1], just after the discovery of the electron, but before that of the proton, as a classical representation of the atom; hence the “plums” representing the electrons, and the introduction of a homogeneous background (the “pudding”), to fulfill electro-neutrality. This picture, although obsolete in the atomic realm, has nevertheless attracted the interest of mathematicians, physicists and biologists alike, due to its relevance in particular for ionic ordering at interfaces [4], for the behaviour of colloids self-assembled at the edge of emulsion droplets (colloidosomes, see, *e.g.*, [5]), for the study of one-component plasmas and their experimental realizations (electrons on a liquid-helium surface [6]) or for understanding viral morphology [7]. The Thomson problem reappeared recently in sheep’s clothing in different contexts, from the screening effects in hydrophobic polyelectrolytes [8], to the behaviour of Coulomb balls (identical particles confined in a harmonic trap [9]), including hydrogels [10], where the uptake of counterions by a cross-linked polymer network (the “pudding”) is the key feature leading to the expansion of the network by osmotic pressure, hence the capability to absorb large quantities of

water. At variance with Thomson’s preoccupation where ground-state configurations were under scrutiny, those articles were concerned with the finite-temperature behaviour ( $T \neq 0$ ). At high to moderate temperatures, mean-field theory provides a trustworthy framework, and allows to obtain some analytical results [8]. The regime of low temperatures (large couplings, a notion to be specified below) is more elusive, and it will be our primary objective in the present contribution. Several analytical predictions will be derived, including scaling laws for two important quantities characterizing the screening properties. These predictions will be tested against numerical simulations, that also give access to detailed microscopic information concerning the structure.

We start by defining the model and introducing a relevant coupling parameter. We consider a single permeable and spherical globule of radius  $R_g$  and charge  $-zqZ_g$  (referred to as the background), surrounded by its  $Z_g$  counterions of charge  $zq$ , where  $q$  is the elementary charge and  $z$  the ionic valency. It should be stressed that the counterions can penetrate but also *leave* the homogeneously charged globule, which is an important difference with Thomson’s original formulation. Without loss of generality, the globule is assumed negatively charged (positive counterions). In such a salt-free system, a confining cell is required to avoid evaporation of all counterions; its radius is denoted  $R_c$ . A key quantity is the “globule total uptake” charge  $-Z_{\text{up}}$ , which includes

the background and the counterions present within the globule<sup>1</sup>. Hence,  $Z_g - Z_{\text{up}}$  can be viewed as the number of counterions outside the globule. Following [9,11], we define the coupling (plasma) parameter  $\Gamma$  as the ratio between the characteristic electrostatic energy of a counterion-counterion interaction,  $z^2 q^2 / (4\pi\epsilon\delta)$ , and the thermal energy,  $kT$ . Here  $\epsilon$  is the solvent dielectric constant, and the distance  $\delta$  is taken as the ion sphere radius:  $Z_g \delta^3 = R_g^3$ . Introducing the Bjerrum length  $\ell_B = q^2 / (4\pi\epsilon kT)$ , which is about 7 Å in water at room temperature, we get

$$\Gamma = \frac{z^2 q^2}{4\pi\epsilon\delta kT} = Z_g^{1/3} \frac{z^2 \ell_B}{R_g}. \quad (1)$$

For  $\Gamma < 1$ , mean-field Poisson-Boltzmann theory [11] provides an accurate description, while the strong-coupling regime corresponds to  $\Gamma > 1$ . It has been shown in [8] that within the non-linear mean-field regime<sup>2</sup>, counterion penetration into the globule leads to  $Z_{\text{up}} \propto \sqrt{Z_g}$  for large enough bare charge  $Z_g$ . For the purpose of comparison with numerical calculations in the strongly coupled regime, this quantity needs suitable rescaling, and we define

$$\Pi = Z_{\text{up}} \frac{z^4 \ell_B^2}{R_g^2}, \quad (2)$$

which only depends on  $\Gamma$  (see footnote <sup>3</sup>). Within mean field, we then have  $\Pi \propto \Gamma^{3/2}$  up to a prefactor of order 1, and in addition, the relation  $n \propto \exp(-ze\phi/kT)$  between counter-ions density  $n(\mathbf{r})$  and the local mean electrostatic potential  $\phi(\mathbf{r})$  [11], allows us to relate the reduced charge  $\Pi$  to the characteristic decay length of  $n(r)$  at  $r = R_g$ . To this end, we define the positive quantity

$$S = -z^2 \ell_B \left. \frac{d}{dr} \right|_{r=R_g} \log n(r), \quad (3)$$

that can be viewed as the reduced (inverse) decay length of the counterion profile in the globule vicinity. Gauss theorem implies  $S = \Pi$ , again within irrelevant prefactors: the reduced decay length  $S^{-1}$  is inversely proportional to the reduced total charge, that is itself an increasing function of the background charge  $Z_g$ .

How are the previous results affected in the strong-coupling regime? To make analytical progress when  $\Gamma \gg 1$ , we take advantage of the caging of particles that takes place under their strong mutual repulsion [12]<sup>4</sup>. This basic

feature of strongly coupled Coulomb or Yukawa plasmas is at the root of the quasi-localized charge approximation, that has proved useful for the determination of dynamic quantities [16]: the charges inside the globule are trapped around local potential minima, and therefore oscillate at a frequency close to the Einstein value  $\omega_E^2 = n_0 z^2 q^2 / (3m\epsilon)$  [17]<sup>5</sup>, where  $n_0 = Z_g / (4\pi R_g^3 / 3)$  is the background density, and  $m$  is the counterion mass. The potential felt locally by a counterion then reads

$$U(x) = \frac{1}{2} \frac{z^2 q^2 n_0}{3\epsilon} x^2 = \frac{1}{6} \frac{kT}{\lambda^2} x^2 \quad (4)$$

where  $x$  stands for the deviation from potential minimum, and  $\lambda = [z^2 q^2 n_0 / (\epsilon kT)]^{-1/2}$  can be thought of as a Debye length. The typical cage size is given by  $\delta$ , as required from local electro-neutrality, and likewise, those cages located near the boundary of the globule ( $r = R_g$ ) are centered at  $r = R_g - \delta_{\text{max}}$ . We expect  $\delta_{\text{max}}$  and  $\delta$  to scale accordingly, and more precisely, we write  $\delta_{\text{max}} = \alpha\delta$ , where  $\alpha$  will be an important quantity for what follows. Due to the repulsion of neighboring counterions, we anticipate  $\alpha < 1$  (the outer layer of confined ions is “pushed” towards the boundary  $r = R_g$ , by a mechanism reminiscent of depletion in hard core systems). This is precisely the scenario at work in the ground state (*i.e.* at infinite  $\Gamma$ ), where several approximate expressions have been proposed for  $\alpha$  [12]. Consistent with these approximations and with numerical simulations that report  $0.73 < \alpha < 0.77$  [12], we will take  $\alpha = 3/4$  for our large-coupling expansions.

We are now in a position to compute the uptake charge of the globule, from the number of counterions that are able to escape their cage. At large  $\Gamma$ , only those cages located near the globule boundary can loose particles; there are  $(R_g/\delta)^2$  such cages, so that

$$Z_{\text{up}} \simeq \frac{R_g^2}{\delta^2} \int_{\delta_{\text{max}}}^{\infty} \frac{dx}{\lambda} \exp\left(-\frac{x^2}{6\lambda^2}\right) \quad (5)$$

$$\simeq \frac{R_g^2}{\delta^2} \frac{\lambda}{\delta_{\text{max}}} \exp\left(-\frac{\delta_{\text{max}}^2}{6\lambda^2}\right). \quad (6)$$

Since  $\delta^2/\lambda^2 = 3z^2 \ell_B/\delta = 3\Gamma$ , and going from  $Z_{\text{up}}$  to its rescaled form  $\Pi$ , we obtain

$$\Pi \propto \Gamma^{3/2} \exp(-\alpha^2 \Gamma/2). \quad (7)$$

This shows, under strong coupling and at variance with mean-field, that the uptake charge actually *decreases* upon increasing the globule charge; furthermore, it is noteworthy that our argument, valid at large  $\Gamma$ , also

<sup>1</sup>We avoid the terminology “effective” for  $Z_{\text{up}}$ , which has a different meaning (charge extracted from the far-field behaviour).

<sup>2</sup>Note that the weak-coupling limit  $\Gamma < 1$  is compatible with strong non-linear effects, which occur within mean field whenever  $Z_g \ell_B / R_g \gg 1$  (which is easily met), provided  $\ell_B \ll R_g$ , see eq. (1).

<sup>3</sup>At large  $\Gamma$ , the particular choice of  $R_c$  does not affect our predictions —as can be seen in fig. 1— as long as it is finite.

<sup>4</sup>A similar phenomenon is at the root of the strong-coupling expansion performed when the macro-ions are *impermeable* to the counterions, that then form a strongly modulated two-dimensional liquid (or even solid at extreme couplings), see, *e.g.*, [11,13–15]. Compared to those works, we are here investigating the *permeable* case where counterions can enter the charged colloids, with a corresponding strongly modulated three-dimensional liquid formation.

<sup>5</sup>If the charges are crystallised on an ordered lattice, harmonic motion occurs with frequency  $\omega = \omega_E$ . For a disordered lattice,  $\omega^2$  is distributed around  $\omega_E^2$  with spread that vanishes at large  $\Gamma$  [17]. Long-range order is not required though, as a similar phenomenon holds for a strongly modulated liquid, the situation we consider here. We therefore emphasize that our approach does not require *stricto sensu* crystallisation, but rather the occurrence of a correlation hole around the counterions present in the globule.

reproduces the mean-field small  $\Gamma$  behaviour with a power law of exponent  $3/2$ .

We now seek a more microscopic information and attempt to predict the radial dependence of the counterion profile  $n(r)$  outside the globule. When a counterion approaches the globule, it polarizes the trapped ions in their cages, and in turn feels the potential  $V(r)$  thereby created (the more obvious  $Z_{\text{up}}/r$  contribution appears to be sub-dominant, see below). More specifically, the test particle located at  $\mathbf{r}$  creates a field  $\mathbf{E} = -zq(\mathbf{r} - \mathbf{x})/(4\pi\epsilon|\mathbf{r} - \mathbf{x}|^3)$  at point  $\mathbf{x}$  where a counterion located inside the globule will be displaced from its equilibrium position, creating a dipole moment  $\mathbf{p} = 3z^2q^2\lambda^2\mathbf{E}/kT$  (see footnote <sup>6</sup>). The contribution of this dipole to the potential  $V$  felt by the test charge is  $\mathbf{p} \cdot (\mathbf{r} - \mathbf{x})/(4\pi\epsilon|\mathbf{r} - \mathbf{x}|^3)$ , an expression that we have to integrate over all cages of counterions (one dipole for each cage); moreover, for consistency with our previous argument with outer cages centered at a radial position  $R_g - \delta_{\text{max}}$ , and gathering expressions, we have

$$V(\mathbf{r}) \simeq -n_0 \frac{3z^3q^3\lambda^2}{(4\pi\epsilon)^2kT} \int_{|\mathbf{x}| \leq R_g - \delta_{\text{max}}} \frac{1}{|\mathbf{r} - \mathbf{x}|^4} d^3\mathbf{x}. \quad (8)$$

To obtain the dominant contribution, in the vicinity of  $R_g$ , we neglect the curvature of the globule, which gives

$$\frac{-zqV(r)}{kT} \propto \frac{\ell_B}{r - R_g + \delta_{\text{max}}} \quad \text{with } r = |\mathbf{r}|. \quad (9)$$

The corresponding density profile follows from  $n(r) \propto e^{-V/kT}$ , which yields the dominant behaviour  $\log n \propto \ell_B/(r - R_g + \delta_{\text{max}})$ . This allows not only to compute the scaling parameter  $S$  but also to propose a scaling function for  $n(r)$ . Indeed we obtain here  $S \propto z^2\ell_B^2/\delta^2$  from the definition (3), *i.e.*  $S \propto \Gamma^2$ , and

$$\frac{1}{\Gamma} \log \frac{n(r)}{n(R_g)} \propto \mathcal{F}(\zeta) = [(\zeta + \alpha)^{-1} - \alpha^{-1}] \quad (10)$$

with  $\zeta = (r - R_g)/\delta$ . As a consequence, if the scaling relation (10) holds, an important test for the consistency of our approach is to recover the same value of  $\alpha$  as in expression (7), close to  $3/4$ . To summarize our analytical findings, we obtained, in addition to the explicit scaling form (10), that while  $\Pi \propto S \propto \Gamma^{3/2}$  in the non-linear mean-field regime (meaning the limit of large bare charges  $Z_g$  within Poisson-Boltzmann theory), strong coupling leads to  $S \propto \Gamma^2$  and an uptake charge (background plus counterions present within the globule)  $\Pi \propto \Gamma^{3/2} \exp(-\alpha^2\Gamma/2)$ . The slope ( $S$ ) increases with  $\Gamma$  steeper than in mean field, and ionic correlation effects lead at large  $\Gamma$  to a decrease of the charge  $\Pi$ .

To put these predictions to the test, we have performed Monte Carlo simulations, where the counterion interact

<sup>6</sup>A simple argument provides the needed polarizability of a cage: for an ion displaced by a quantity  $\delta\mathbf{r}$  from its equilibrium position by an external field  $\mathbf{E}$ , we have the force balance condition  $m\omega_E^2\delta\mathbf{r} = zq\mathbf{E}$ , which yields the dipole moment  $\mathbf{p} = zq\delta\mathbf{r} = z^2q^2\lambda^2\mathbf{E}/(kT)$ .

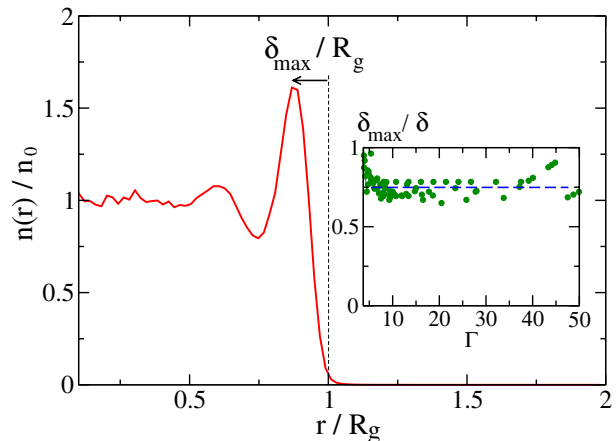


Fig. 1: (Colour on-line) Counterion density profile  $n$  normalized by background density  $n_0$  as a function of distance from the globule center (normalized by the globule radius  $R_g$ ). Here  $\Gamma = 13$ ,  $R_c/R_g = 2$  and  $Z_g = 200$ . The density peak location defines the distance  $\delta_{\text{max}}$ , that is shown in the inset at various couplings, different cell radii ( $R_c/R_g = 2, 4$  and  $8$ ) and  $Z_g$  from 50 to 3000. The dashed line shows the value  $3/4$ , used for  $\alpha$  throughout this work.

through the exact Coulomb law and feel the background charge of the globule, the whole system being furthermore enclosed in a larger sphere of radius  $R_c$  (see footnote <sup>3</sup>). Following the analytical treatment, we located the position of counterionic density peak close to the globule edge, which defines  $\delta_{\text{max}}$ , see fig. 1. The inset of this figure shows that the ratio  $\alpha = \delta_{\text{max}}/\delta$  does not depend on the coupling strength, and remains close to its ground-state limit  $\alpha \simeq 3/4$ . Recovering the proper value of  $\alpha$  at large  $\Gamma$  can be viewed as an assessment of the validity of our simulations, and we can then proceed with the explicit check of the scaling form eq. (10). It can be seen in fig. 2 that the different curves exhibit good collapse at different  $\Gamma$ , and that the function  $\mathcal{F}(\zeta)$  captures the density decay in the external vicinity of the globule ( $\zeta > 0$ ). While our argument above only provides the relation  $\Gamma^{-1} \log[n(r)/n(R_g)] \propto \mathcal{F}(\zeta)$ , a more refined analysis indicates that the prefactor is close to  $1/2$  [18], so that we have plotted  $\mathcal{F}(\zeta)/2$  in fig. 2. We have also computed the values of  $S$  and  $\Pi$  in the simulations. They are shown in fig. 3, which fully corroborates the analytical scaling behaviours. First, at small  $\Gamma$ , we have the mean-field behaviour  $S \propto \Pi \propto \Gamma^{3/2}$ , while at larger couplings,  $S \propto \Gamma^2$  and  $\Pi$  becomes non-monotonous. The detailed behaviour of  $\Pi$  *vs.*  $\Gamma$  provides a stringent test for our arguments: as shown in the inset of fig. 3, the dependence of  $\log(\Pi/\Gamma^{3/2})$  on  $\Gamma$  is linear at large  $\Gamma$ , with a (negative) slope compatible with the predicted value of  $\alpha^2/2 = 9/32$ . We see that a unique value of  $\alpha$ , inherited from ground-state properties, accounts for the behaviour of the density profile together with more global quantities like the uptake charge.

The previous considerations provide a detailed description for the ionic density profile outside the globule. The

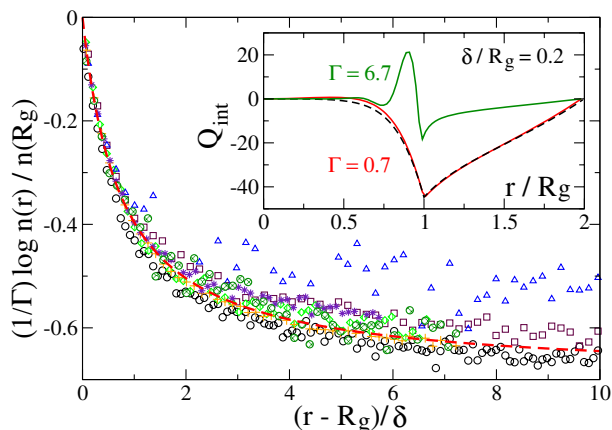


Fig. 2: (Colour on-line) Plots of rescaled counterion profiles in the vicinity of the globule,  $\Gamma^{-1} \log[n(r)/n(R_g)]$ , as a function of  $\zeta = (r - R_g)/\delta$ . The different symbols correspond to different values of  $\Gamma$ , from 8 to 24. The thick dashed curve is for the function  $\mathcal{F}(\zeta)/2$ , where  $\mathcal{F}$  is defined in eq. (10), with a value  $\alpha = 3/4$ . Inset: integrated charge  $Q_{\text{int}}$  vs. radial distance, at weak and strong couplings. For  $\Gamma < 1$ ,  $Q_{\text{int}}$  is always of the same sign as the background, while over-charging is observed at strong couplings. The dashed line shows the mean-field result.

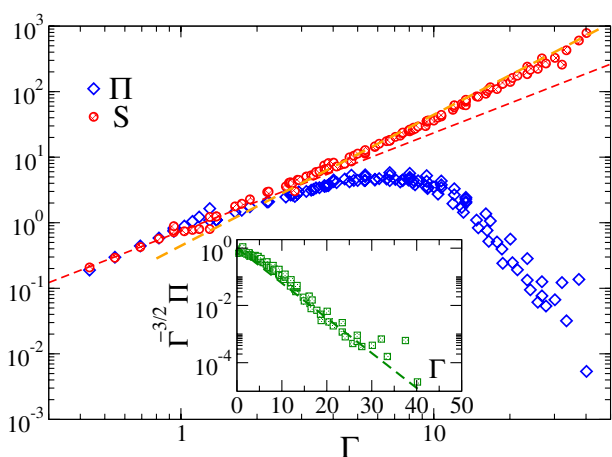


Fig. 3: (Colour on-line) Rescaled counterion density slope  $S$  defined in eq. (3), and reduced uptake charge  $\Pi = Z_{\text{up}} z^4 \ell_B^2 / R_g^2$ , as a function of coupling parameter  $\Gamma$ . The dashed lines have slope  $3/2$  (to evidence the mean-field behaviour) and  $2$ . Here  $S$  has been divided by  $2$  to have  $S \simeq \Pi$  at low  $\Gamma$ . The inset shows  $\Pi/\Gamma^{3/2}$  as a function of coupling, on a linear-log scale. The line has slope  $-\alpha^2/2 \simeq -0.28$ .

behaviour for  $r < R_g$  is more intricate, and has been analyzed in Monte Carlo. A quantity of interest is the total integrated charge  $Q_{\text{int}}(r)$  inside a sphere of radius  $r$ . By definition,  $Q_{\text{int}}(R_g) = -Z_{\text{up}}$  and  $Q_{\text{int}}(R_c) = 0$  due to electro-neutrality. Within mean field, it is interesting to note that  $Q_{\text{int}}$  is always of the same sign as the background (here, negative). One can also note that the salt-free nature of our system imposes  $Q_{\text{int}}(R_g) < 0$ , and more precisely, that  $Q_{\text{int}}(r) < 0$  for all  $r \geq R_g$ . Hence,

a true overcharging cannot be observed in our salt-free system [11,13]. However, for  $\Gamma > 1$ , the inset of fig. 2 shows that  $Q_{\text{int}}(r)$  exhibits a range of distances where it is positive: we refer to such a possibility as a *local* over-charging, and we note that it is somehow reminiscent of its counterpart occurring for impermeable colloids [11,13]. Indeed, as for impermeable colloids, it is possible to prove that local overcharging is precluded within mean-field theories [18,19], so that when present, it is a manifestation of ionic correlations, that become prevalent at  $\Gamma > 1$ . The electrophoretic consequences of this over-charging effect are unclear, and left for future study. Incidentally, the close agreement between Monte Carlo and mean-field results at small  $\Gamma$  (see inset of fig. 2) can be seen as assessing the validity of the numerical methods employed.

To summarize, we investigated the screening properties of a uniformly charged spherical globule, neutralized by point counterions. Invoking a quasi-localized charge argument at strong Coulombic coupling  $\Gamma$ , we obtained analytically the counterion density profile  $n(r)$  outside the globule, together with two more global quantities: one, denoted  $S$ , follows from  $n(r)$  and is its characteristic inverse decay length in the globule edge vicinity ( $r = R_g$ ); the second quantity,  $\Pi$ , stands for the reduced total charge inside the globule and quantifies the counterion uptake. At small couplings,  $S$  and  $\Pi$  coincide and scale as  $\Gamma^{3/2}$ . Strong ionic correlations, on the other hand, were shown to lead to a departure of both quantities: the slope  $S$  becomes steeper (algebraic increase in  $\Gamma^2$ ) and the counterion uptake is much more efficient, leading to a charge  $\Pi$  that *decreases* upon increasing  $\Gamma$  (which can be obtained increasing the globule bare charge  $Z_g$ ): the algebraic mean-field increase turns into an exponential decrease, see eq. (7). Our scaling predictions are free of adjustable parameters, and make use of known ground-state properties [12] (that fix the parameter  $\alpha = \delta_{\text{max}}/\delta$ ). These predictions were corroborated by Monte Carlo simulations, that provide the exact static properties of our system at arbitrary  $\Gamma$ , and that furthermore revealed an over-charging effect that is absent within the mean-field scenario. We have treated the phenomenon of caging at a rather simple level, that turns out to be sufficient to capture the interesting violations of mean field, driven by ionic correlations. In addition, while the mean-field theory applies schematically for  $\Gamma < 1$  and the strong-coupling arguments cover the range  $\Gamma > 10$ , a quantitative understanding of the crossover region at moderate couplings presumably requires intermediate approaches in the spirit of refs. [20].

Our work opens interesting venues for future studies. First, our predictions can be tested experimentally, in the spirit of the experiments reported in [21]. For the corresponding hydrophobic polyelectrolytes, we estimate that  $\Gamma \simeq z^2$  at room temperature, where  $z$  is the valency of the counterions. Consequently, with trivalent ions, one has  $\Gamma \simeq 9$ , which is the regime where mean field no longer applies, and our strong-coupling predictions



take over, see fig. 3. Second, the phase behaviour of an ensemble of such globules is unknown, together with the effects of an added electrolyte. Finally, the response to external perturbations, both static (sedimentation) or dynamic (electrophoresis), should provide a relevant ground to investigate the signature of strong Coulombic correlations.

## REFERENCES

- [1] THOMSON J. J., *Philos. Mag.*, **7** (1904) 237.  
 [2] SAFF E. B. and KUIJLAARS A. B. J., *Math. Intell.*, **19** (1997) 5; ALTSCHULER E. L. *et al.*, *Phys. Rev. Lett.*, **78** (1997) 2681.  
 [3] For variants of the original problem, see, *e.g.*, BOWICK M., CACCIUTO A., NELSON D. R. and TRAVESSET A., *Phys. Rev. Lett.*, **89** (2002) 185502; LEVIN Y. and ARENZON J. J., *Europhys. Lett.*, **63** (2003) 415; SLOSAR A. and PODGORNIK R., *Europhys. Lett.*, **75** (2006) 631.  
 [4] LEIDERER P., *Z. Phys. B*, **98** (1993) 303.  
 [5] DINSMORE A. D., HSU M. F., NIKOLAIDES M. G., BAUSCH A. R., MARQUEZ M. and WEITZ D. A., *Science*, **298** (2002) 1006.  
 [6] MONARKHA Y. and KONO K., *Two-Dimensional Coulomb Liquids and Solids* (Springer, Berlin) 2004.  
 [7] CASPAR D. L. D. and KLUG A., *Cold Spring Harbor Symp. Quant. Biol.*, **27** (1962) 1.  
 [8] CHEPELIANSKII A., MOHAMMAD-RAFIEE F., TRIZAC E. and RAPHAEL E., *J. Phys. Chem. B*, **113** (2009) 3743.  
 [9] WRIGHTON J., DUFTY J. W., KAHLERT H. and BONITZ M., *Phys. Rev. E*, **80** (2009) 066405.  
 [10] CLAUDIO G. C., KREMER K. and HOLM C., *J. Chem. Phys.*, **131** (2009) 094903.  
 [11] LEVIN Y., *Rep. Prog. Phys.*, **65** (2002) 1577.  
 [12] HASSE R. W. and AVILOV V. V., *Phys. Rev. A*, **44** (1991) 4506; see also CIOSLOWSKI J. and GRZEBIELUCHA E., *Phys. Rev. E*, **78** (2008) 026416.  
 [13] SHKLOVSKII B. I., *Phys. Rev. E*, **60** (1999) 5802.  
 [14] BOROUDJERDI H., KIM Y.-W., NAJI A., NETZ R. R., SCHLAGBERGER X. and SERR A., *Phys. Rep.*, **416** (2005) 129.  
 [15] ŠAMAJ L. and TRIZAC E., *Phys. Rev. Lett.*, **106** (2011) 078301.  
 [16] DONKÓ Z., KALMAN G. J. and GOLDEN K. I., *Phys. Rev. Lett.*, **88** (2002) 225001; KALMAN G. J., GOLDEN K. I., DONKÓ Z. and HARTMANN P., *J. Phys.: Conf. Ser.*, **11** (2005) 254.  
 [17] BAKSHI P., DONKÓ Z. and KALMAN G. J., *Contrib. Plasma Phys.*, **43** (2003) 261.  
 [18] CLOSA F., CHEPELIANSKII A., RAPHAËL E. and TRIZAC E., in preparation.  
 [19] TRIZAC E., *Phys. Rev. E*, **62** (2000) R1465.  
 [20] BURAK Y., ANDELMAN D. and ORLAND H., *Phys. Rev. E*, **70** (2004) 016102; CHEN Y. G. and WEEKS J. D., *Proc. Natl. Acad. Sci. U.S.A.*, **103** (2006) 7560; SANTANGELO C. D., *Phys. Rev. E*, **73** (2006) 041512; BUYUKDAGLI S., MANGHI M. and PALMERI J., *Phys. Rev. Lett.*, **105** (2010) 158103.  
 [21] ESSAFI W., LAFUMA F., BAIGL D. and WILLIAMS C. E., *Europhys. Lett.*, **71** (2005) 938.